

A Climate Sensitivity Study by Use of a Coupled Atmosphere-Ocean Model

Contact Person Tatsushi Tokioka
Climate Research Department, Meteorological Research Institute

Research Organization Akira Noda, Tatsuo Motoi, Seiji Yukimoto,
Akio Kitoh, Yoshinobu Nikaidou, Masahide Kimoto
Climate Research Department, Meteorological Research Institute

Keywords climate model, climate change, global warming

1. Introduction

Recent study on global warming by use of coupled ocean-atmosphere general circulation model (CGCM) has shown that oceans substantially influence the timing and patterns of climate change, mainly, through the vertical mixing of heat between the surface layer and deeper layers.¹⁻² The influence is particularly pronounced in the circumpolar ocean of the Southern Hemisphere and in the northern North Atlantic. In these region, sea ice plays an important role for the vertical mixing, but simulations of sea ice have been quite unsatisfactory yet.

On the other hand, it has been well known that the sea-surface temperature (SST) anomalies due to El Niño-Southern Oscillation (ENSO) in the tropics have a great impact on seasonal climate not only over tropics but also in the extratropics through teleconnections. Nagai et al.³ successfully simulated the ENSO phenomenon but they required an ocean model which has a finer resolution than those so far used for global warming.

There remains, therefore, much to be done to predict global climate change. We have been developing a CGCM to study global climate change and climate sensitivity. The purpose of the present study is to simulate a present climate and then to evaluate the climate sensitivity on a gradual increase in CO₂ by using the CGCM developed at the MRI (Meteorological Research Institute). The ocean part of the CGCM has finer resolutions in the tropics so that the model can simulate ENSO phenomenon. Since the computation is now continuing, we will briefly describe the CGCM and present preliminary results. We hope that this study will make a contribution to the forthcoming IPCC (Intergovernmental Panel on Climate Change) report.

2. Description of the model

The CGCM used for this study consists of a general circulation model of the world oceans (OGCM) coupled to a general circulation model of the atmosphere (AGCM) with a sea-ice model and a land surface model, developed at the MRI. The method how to couple the models is an important part for climate modeling. It controls the exchange of momentum, heat and water fluxes between atmosphere and ocean and then influences

the simulated fields of the model. Each component of the CGCM and the method of coupling will be described in this section.

2.1. Atmospheric model

The AGCM is a new version of MRI-GCM. The earlier version is described in Tokioka et al.⁴ in detail. Subsequent modifications include increases in the vertical resolution, and changes in parameterizations of gravity-wave drag, atmospheric radiation, convection, surface characteristics, and land surface processes. Only the main modifications will be described here.

The horizontal resolution of the AGCM is 4°×5° latitude/longitude grid. In order to allow different horizontal resolutions between AGCM and OGCM, different types of surface characteristics (ocean, land, sea ice and ice sheet) are considered in a single AGCM grid cell. The fractional rate of land coverage of the AGCM grid points is shown in Fig. 1.

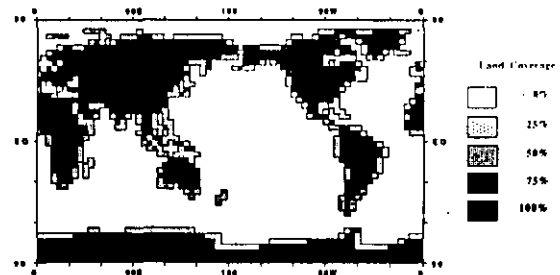


Fig. 1 The fractional rate of land coverage (%) of the AGCM grid points.

The vertical resolution is 15 hybrid levels between surface to model top at 1hPa. Above 100hPa log-pressure coordinates, and below 100hPa modified sigma coordinates are used. The vertical structure of the AGCM is shown in Fig. 2.

Orographic gravity-wave drag is simulated following Palmer et al.⁵ with quantitative adjustments described by Yagai and Yamazaki.⁶ Parameterization of cumulus convection is based on the scheme of Arakawa and Schubert.⁷ The scheme predicts mass fluxes from mutually interacting cumulus subensembles which have different entrainment rates and cloud top. The Arakawa-Schubert

scheme is modified⁸ to impose an additional constraint between the minimum entrainment rate and the depth of the predicted PBL layer.

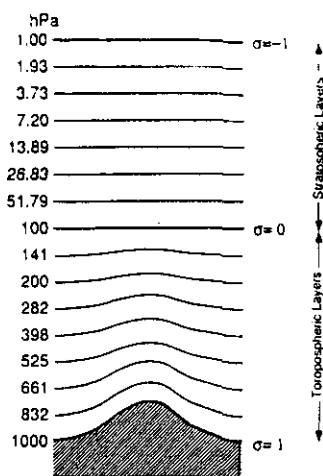


Fig. 2 The vertical structure of the AGCM.

Five types of cloud are simulated: penetrative cumulus cloud, mid-level convective cloud, PBL stratus cloud, large-scale condensation cloud, and cirrus anvil cloud. Partial cloudiness is allowed for the convective clouds.

The calculation of shortwave radiation follows the method of Lacis and Hansen.⁹ Rayleigh scattering and absorption by ozone, water vapor and carbon dioxide are calculated. The calculations of longwave radiation are based on the multiparameter random model by Shibata and Aoki¹⁰ applied in four spectral regions (20-550, 550-800, 800-1200, 1200-2200 cm^{-1}). Absorption bands of carbon dioxide, ozone and water vapor, and continuum absorption by water vapor are treated.

Thermodynamic and hydrological treatment of land surface are based on multi-layer soil model. The model has four layers with the bottom at 10 m depth. Ground temperature, soil moisture and frozen soil moisture are predicted at each level. The melt of frozen soil of tundra in case of global warming is taken into account. The effects of vegetation canopy are not explicitly modeled.

2.2. Ocean model

The ocean model is a world ocean general circulation model developed at the MRI. It follows basically the ocean general circulation model of Bryan.¹¹ The Mellor and Yamada¹² level 2 turbulence closure scheme is included to improve the simulations of the ocean mixed layer.

The physical condition of the ocean is specified by seven variables, velocity (u, v and w), pressure (P), in-situ density (ρ), potential temperature (T), and salinity (S) in the model. The model employs the Boussinesq and rigid-lid approximations and hydrostatic assumption. The governing equations of the model are momentum equations, the mass

continuity equation, the conservation equations for heat and salt, and the equation of state.

The convective adjustment is employed for T and S such that statically unstable water is mixed to neutral stratification. The equation of state for in-situ density from in-situ temperature¹³ and the Fofonoff's procedure for calculating in-situ temperature from potential temperature are combined to give a function for in-situ density.

The lateral eddy viscosity and diffusivity are set to be $2.0 \times 10^9 \text{ cm}^2/\text{s}$ and $5.0 \times 10^7 \text{ cm}^2/\text{s}$, respectively, between 78°N and 78°S . Smaller values are used in other area, corresponding to the smaller zonal grid distance near the poles.

The vertical eddy viscosity and diffusivity are calculated following Mellor and Yamada^{12,14} and Mellor and Durbin,¹⁵ the minimum values of which are introduced ($1.0 \text{ cm}^2/\text{s}$ and $0.5 \text{ cm}^2/\text{s}$, respectively) to guarantee subgrid-scale mixing.

The bottom friction is formulated based on the Ekman boundary layer theory with $1.0 \times 10^2 \text{ cm}^2/\text{s}$ for the coefficient of the vertical eddy viscosity in the bottom Ekman layer.

The method for calculation of the stream function with many isolated continents and islands has been originally proposed by Kamenkovich¹⁶ and extended to the time-dependent problem by Bryan¹¹ and Bryan and Cox.¹⁷ The same method is introduced in the model to obtain the time tendency of the stream function. In the Arctic Ocean (poleward of 82°N) only, pressure gradient as well as mass divergence is smoothed longitudinally to avoid a computational restriction on the time step because of the small geographical distances in the longitudinal direction. The method of smoothing follows the idea proposed by Arakawa.¹⁸

The governing equations, along with their boundary conditions, are solved by finite difference techniques with a staggered "B" grid configuration. The finite difference scheme is energetically consistent and is of second-order accuracy in space and time. A formulation of finite differencing for diagonally upward (downward) advection of momentum at the bottom slope is newly introduced in the model. Since the vertical diffusion of momentum, heat and salt are split and expressed by implicit scheme, small vertical spacing is permissible near the surface without reducing the time increment nor restricting the magnitude of the mixing coefficients. The integration for vertical diffusion proceeds through tri-diagonal matrix reduction technique.

The horizontal grid spacing is 2° latitude \times 2.5° longitude in the global domain. The equatorial region between 12°N and 12°S uses finer latitudinal resolutions with $1/2^\circ$ within 4°N - 4°S band and almost linearly varying grid spacing from $1/2^\circ$ to 2° between 4°N(S) and 12°N(S) . The vertical layers vary in thickness to have finer resolutions near the surface. There are 21 layers, which thicken from 5.2m at the surface to 700m at 5000m depth, with eleven layers in the top 300m. The vertical structure of the OGCM is shown in Fig. 3. The

bottom topography and coast lines are realistically included on a scale consistent with the resolutions (Fig. 4). The maximum ocean depth is taken as 5000m.

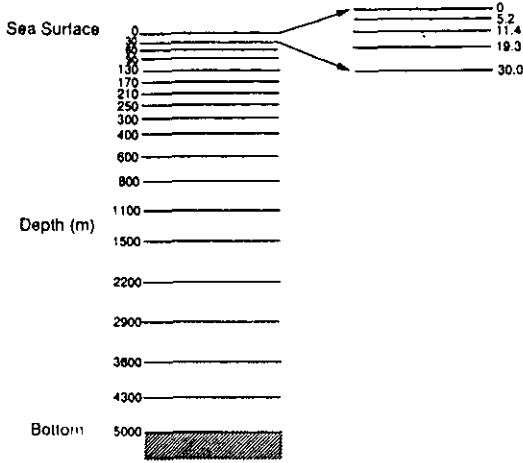


Fig. 3 The vertical structure of the OGCM.

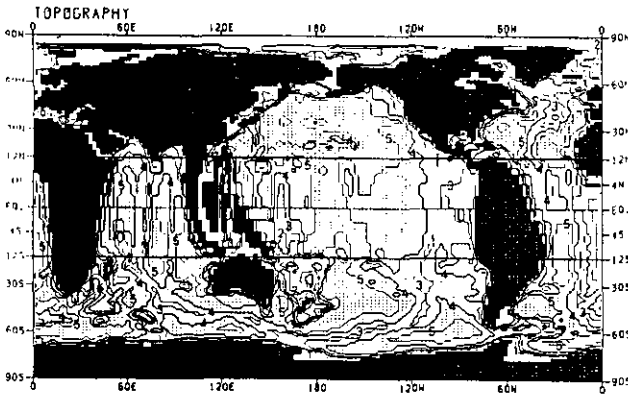


Fig. 4 The horizontal resolutions and the topography of the OGCM.

2.3. Sea-ice model

The sea-ice model is developed at the MRI based on modeling ideas of Mellor and Kantha.¹⁹ The prognostic variables of the present model are sea-ice thickness h_i and sea-ice concentration A . The model consists of the equation of mass,

$$\begin{aligned} \frac{\partial (Ah_i)}{\partial t} + Ah_i \text{div} \mathbf{u}_{\text{eff}} \\ = \frac{\rho_0}{\rho_i} [A(W_{IO} + W_{AI}) + (1-A)W_{AO} + W_{FR}] \\ + \text{Diffusion} \end{aligned} \quad (1)$$

and the equation of sea-ice concentration,

$$\begin{aligned} \frac{\partial A}{\partial t} + A \text{div} \mathbf{u}_{\text{eff}} \\ = \frac{\rho_0}{\rho_i h_i} [\Phi(1-A)W_{AO} + \Psi A W_{IO} H(-W_{IO}) \\ + (1-A)W_{FR}] + \text{Diffusion} \end{aligned} \quad (2)$$

where t is the time, \mathbf{u}_{eff} the effective surface current velocity, H the Heaviside step function, W_{IO} the freeze or melt rate at the bottom of the ice, W_{AO} the freeze rate in leads (open water), W_{FR} the rate of ice accretion at the sea surface due to frazil ice formation in the ocean, W_{AI} the melt rate at the top of the ice (see Fig. 5).

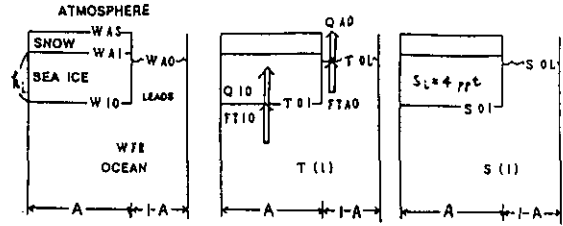


Fig. 5 The structure of the sea-ice model.

The rate of snow melt or accumulation due to precipitation, W_{AS} , and W_{AI} are estimated in the atmospheric component of the CGCM. W_{IO} is calculated from the heat and water balance and equilibrium condition of freezing at the bottom of ice:

$$FTIO = \rho_0 C_p K_T \{T(1) - T_{0I}\}, \quad (3)$$

$$T_{0I} = -0.0543 S_{0I}, \quad (4)$$

$$W_{IO} = (Q_{IO} - FTIO) / \rho_0 L, \quad (5)$$

$$K_S \{S(1) - S_{0I}\} = W_{IO} \{S_i - S(1)\}, \quad (6)$$

where S_{0I} and T_{0I} are salinity and temperature at the bottom of ice, and $FTIO$ is the heat flux to the bottom of ice in the ocean (oceanic heat flux beneath sea ice) (Fig. 5). W_{AO} is predicted from the heat and water balance and freezing relation at the surface of leads:

$$FTAO = \rho_0 C_p K_T \{T(1) - T_{0L}\}, \quad (7)$$

$$T_{0L} = -0.0543 S_{0L}, \quad (8)$$

$$W_{AO} = (Q_{AO} - FTAO) / \rho_0 L, \quad (9)$$

$$K_S \{S(1) - S_{0L}\} = W_{AO} \{S_i - S(1)\}, \quad (10)$$

where S_{0L} and T_{0L} are variables of salinity and temperature at the surface of leads, and $FTAO$ is heat flux to the lead surface in the ocean (oceanic heat flux at leads) (Fig. 5). The heat flux through ice Q_{IO} and the heat flux from the ocean to the atmosphere at leads Q_{AO} , which play a role as thermal forcing in the sea-ice model, are calculated in the atmospheric component of the CGCM. The salinity of sea-ice is taken as 4 ppt.

If the sea water becomes supercooled, frazil ice forms in the ocean and the temperature and salinity of sea water returns to the values T_2 and S_2 , respectively, which satisfy the freezing condition. T_2 , S_2 and the ratio γ of increment mass of frazil

ice to total sea-water mass are estimated from the heat and water balance and freezing condition:

$$T_2 = -0.0543S_2 - 0.000759z, \quad (11)$$

$$C_{p0}T_1 + L = (1 - \gamma)(C_{p0}T_2 + L) + \gamma C_{pi}T_2, \quad (12)$$

$$S_1 = (1 - \gamma)S_2 + \gamma S_i. \quad (13)$$

where T_1 and S_1 are temperature and salinity of supercooled sea water, respectively. The frazil ice is immediately removed from the ocean and added to the ice. The rate of frazil ice accumulation at the sea surface is then

$$W_{FR} = \frac{1}{\Delta t} \int_{-H}^0 \gamma dz \quad (14)$$

where Δt is the time step and H the depth of the ocean.

In the present experiment, u_{eff} and the empirical constants Φ and Ψ in Eqs. (1) and (2) is set as one third of the velocity of the uppermost ocean layer, 1.0 and 0.7, respectively.

2.4. Method of coupling atmosphere, ocean and sea-ice models

In order to take account of the fractional coverage of a single AGCM grid cell with ocean, land, sea ice and ice sheet, momentum, heat and water fluxes at the surface are calculated separately for each surface type in the cell and their area mean fluxes are used to drive atmosphere as lower boundary conditions.

A simple river runoff model is included in the coupling process. Runoff from each land grid is added instantly as fresh water flux to the grid of the river mouth of its basin. Presently, however, fresh water flux due to ablation of ice sheet is not taken into account.

The surface fluxes of heat, momentum and fresh water calculated in the AGCM are interpolated to OGCM grids, averaged over 6 hours and supplied to the OGCM as the upper boundary conditions. The sea surface temperature, sea-ice compactness, sea-ice thickness and temperature of sea-ice bottom which are updated by the time integration of the OGCM and the sea-ice model are transferred to the AGCM every 6 hours.

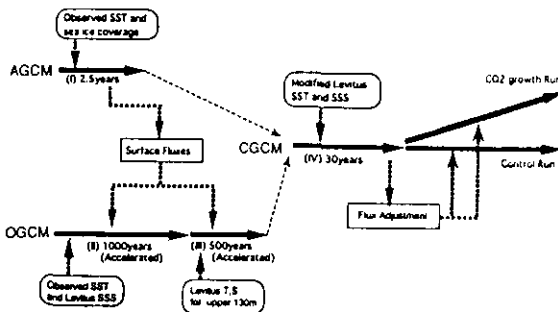


Fig. 6 Diagram which illustrates the succession of experiments being conducted in the present study.

In order to obtain an equilibrium state of the coupled ocean-atmosphere system, four stages of preliminary time integration were performed. Figure 6 illustrates the procedure. In the first stage, the AGCM was run for 3 years forced by the observed SST and sea-ice coverage initiated from the observed state of 1981. The surface fluxes of turbulent heat, radiation, fresh water and momentum obtained from this AGCM-run were stored. In the second stage, the OGCM was integrated with an acceleration method for 1000 years initiated from a steady state with a uniform temperature, using the surface fluxes obtained from the first stage as the upper boundary conditions. The temperatures and salinities of the uppermost layer are relaxed toward the SST used in the first stage and seasonally varying sea surface salinity compiled by Levitus,²⁰ respectively. In the third stage, the OGCM time integration were continued under the same condition as the second stage except for increasing the relaxation layers from top to 130 m depth.

A 30 year time integration of CGCM was performed, as the final stage of the preliminary time integration, initiated from the last states of the AGCM-run and the OGCM-run. Through this integration, relaxation terms for temperature and salinity were stored to be used as flux adjustment to avoid climate drift in the control run and the transient CO₂ run. As an initial condition for the sea-ice model, observed data (averaged over 1981-1983) were used for sea-ice compactness and sea-ice thickness was estimated from compactness.

Currently we are continuing a transient CO₂ experiment with the CGCM. Since we have not obtained definite results from it yet, we will show some preliminary results obtained from the 30 year time integration in the next section.

3. Preliminary Results

The seasonal variations of sea-ice thickness and concentration are reproduced realistically with the CGCM. This means that the boundary conditions for the AGCM is very similar to those of climatology because the SSTs are relaxed to climatological values. Indeed, no significant differences can be found between the present run and the AMIP (Atmospheric Model Intercomparison Project) run where the observed SST and sea-ice extent from 1979 to 1988 were prescribed.

However, even if the SSTs were relaxed to the climatological values, the simulation of sea-ice is very sensitive to model bias because the ice volume is not uniquely determined by the SST. Figures 7 compares the observed and simulated ice concentration for the months of maximum and minimum sea-ice extent in the Northern Hemisphere, and Fig. 8 in the Southern Hemisphere.

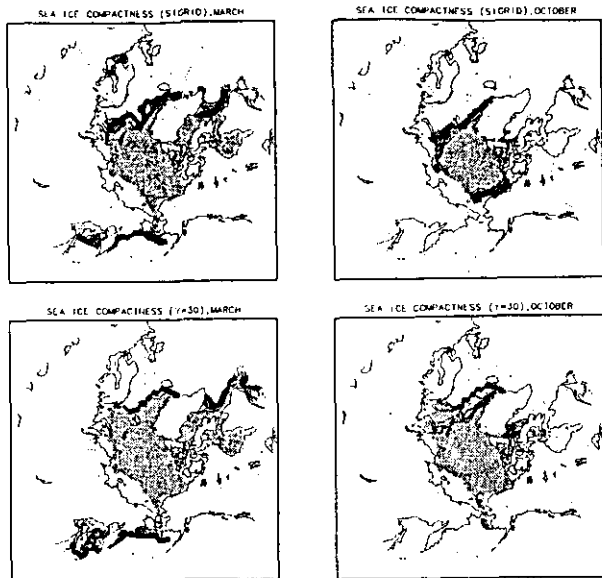


Fig. 7 The observed (upper) and simulated (lower) ice concentration for the months of maximum (right) and minimum (left) sea-ice extent in the Northern Hemisphere. The contour intervals are 10%.

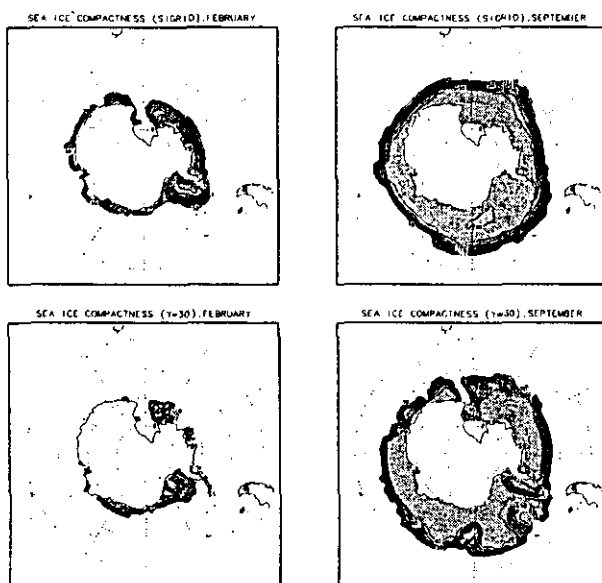


Fig. 8 As in Fig. 8 but for the Southern Hemisphere.

The sea-ice is rather well simulated in the Northern Hemisphere, while a lesser sea-ice extent is simulated for the month of minimum sea-ice extent in the Southern Hemisphere.

The interannual variation of sea-ice compactness and thickness around the north pole and in the Circumpolar Ocean in the Southern Hemisphere can be seen in Figs. 9 and 10, respectively, where

the results for the last ten years of the time integration are shown. Interannual variations can be clearly seen in Fig. 9.

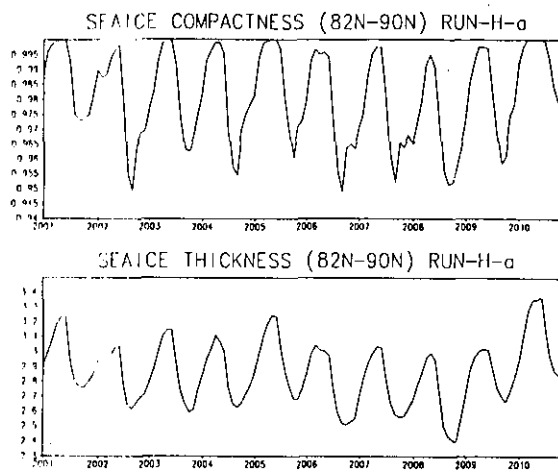


Fig. 9 Annual variation of the sea-ice compactness (upper; unit %) and thickness (lower; unit m) averaged over 82°N-90°N. The results for the last 10 years of the simulation are shown.

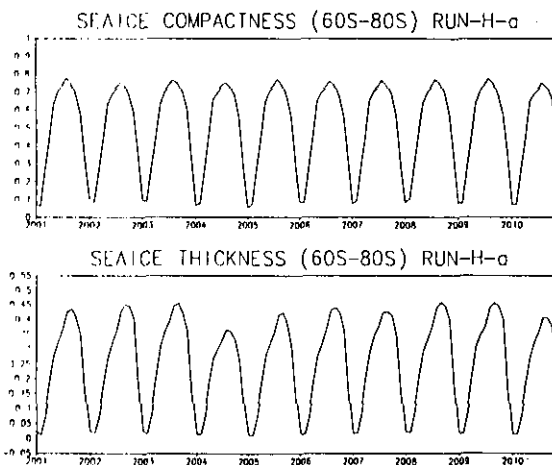


Fig. 10 As in Fig. 9 but for averaged over 60°S-80°S.

4. Summary

The coupled atmosphere-ocean general circulation model (CGCM) and its components, AGCM, OGCM and sea-ice model, developed at the MRI, are described. The OGCM has been integrated to reach an equilibrium state representing the present climate. The OGCM is coupled to the AGCM and sea-ice model to evaluate the flux adjustment which required for the CGCM to simulate the present climate. Some preliminary results obtained from this time integration are presented focussing on the sea-ice. An time integration of the CGCM is now being

undertaken by gradually increasing the atmospheric CO₂.

Acknowledgments

The authors are very grateful to the CGER supercomputer committee for allocating sufficient computing time. Special thanks are extended to staff members of the NIES computer center for their assistance in running the CGCM.

References

1. IPCC,1990: Climate Change; The IPCC Scientific Assessment. eds. J.T. Houghton, G.J. Jenkins and J.J. Ephraums, Cambridge Univ. Press, 365pp.
2. IPCC,1992: Climate Change; The Supplementary Report to The IPCC Scientific Assessment. eds. J.T. Houghton, B.A. Callander and S.K. Varney, Cambridge Univ. Press, 200pp.
3. T. Nagai, T. Tokioka, M. Endoh and Y. Kitamura, 1992: El Niño-Southern oscillation simulated in an MRI atmosphere-ocean coupled general circulation model. *J. Climate*, 5, 1202-1223.
4. T. Tokioka, K. Yamazaki, I. Yagai and A. Kitoh, 1984: A description of the Meteorological Research Institute atmospheric general circulation model (MRI-GCM-I). Tech Report No. 13, MRI, Japan, 249pp.
5. T.N. Palmer, G.J. Shutts, R. Swinbank, 1986: Alleviation of a systematic westerly bias in general circulation and numerical weather prediction models through an orographic gravity wave drag parameterization. *Quart. J. Roy. Meteor. Soc.*, 112, 1001-1031.
6. I. Yagai and K. Yamazaki, 1988: Effect of the initial gravity wave drag on the 12-layer MRI GCM January simulation. Report No. 12 of the 19-23 September 1988 Workshop on Systematic Errors in Models of the Atmosphere, CAS/JSC Working Group on Numerical Experimentation, Toronto, Canada, 8pp.
7. A. Arakawa and W.H. Schubert, 1974: Interaction of a cumulus cloud ensemble with the large scale environment, Part I, *J. Atmos. Sci.*, 31, 674-701.
8. T. Tokioka, K. Yamazaki, A. Kitoh and T. Ose, 1988: The equatorial 30-60 day oscillation and the Arakawa-Schubert penetrative cumulus parameterization. *J. Meteor. Soc. Japan*, 66,883-901.
9. A.A. Lacis and J.E. Hansen, 1974: A parameterization for the absorption of solar radiation in the Earth's atmosphere. *J. Atmos. Sci.*, 31, 118-113.
10. K. Shibata and T. Aoki, 1989: An infrared radiative scheme for the numerical models of weather and climate. *J. Geophys. Res.*, 94, 14923-14943.
11. K. Bryan, 1969: A numerical method for the study of the circulation of the world ocean. *J. Comput. Phys.*, 4,347-376.
12. G.L. Mellor and T. Yamada, 1974: A hierarchy of turbulence closure models for planetary boundary layers. *J. Atmos. Sci.*, 31, 1791-1806.
13. UNESCO, 1981: Tenth Report of the Joint Panel on Oceanographic Tables and Standards. UNESCO Technical Papers in Marine Sci. No. 36. UNESCO, Paris.
14. G.L. Mellor and T. Yamada, 1982: Development of a turbulence closure model for geophysical fluid problems. *Rev. Geophys. Space Phys.*, 20, 851-875.
15. G.L. Mellor and P.A. Durbin, 1975: The structure and dynamics of the ocean surface mixed layer. *J. Phys. Oceanogr.*, 5, 718-728.
16. V.M. Kamenkovich, 1962: On the theory of the antarctic circumpolar current. *Trudy Instituta Okeanologii, Akad. Nauk SSSR*, 56, 245-301.
17. K. Bryan and M.D. Cox, 1972: The circulation of the world ocean: A numerical study. Part I, A homogeneous model. *J. Phys. Oceanogr.*, 2, 319-335.
18. A. Arakawa, 1972: Design of the UCLA general circulation model. Technical Report No. 7, UCLA, 116pp.
19. G.L. Mellor and L. Kantha, 1989: An ice-ocean coupled model. *J. Geophys. Res.*, 94, 10,937-10,954.
20. S. Levitus, 1982: Climatological Atlas of the World Oceans, NOAA Prof. Pap. 13, U.S. Government Printing Office, Washington, D.C..